Geomechanics and Engineering, *Vol. 18, No. 4 (2019) 363-371*
DOI: https://doi.org/10.12989/gae.2019.18.4.363

Effects of rock-support and inclined-layer conditions on load carrying behavior of piled rafts

Yanghoon Roh[1,2], Garam Kim[1], Incheol Kim[1] and Junhwan Lee*[1]

[1]*School of Civil and Environmental Engineering, Yonsei University, 50 Yonsei-ro, Seodaemun-gu, Seoul 03722, Republic of Korea*
[2]*Geotechnical and Tunnel Division, Dohwa Engineering Co., LTD., 438 Samseong-ro, Gangnam-gu, Seoul 06178, Republic of Korea*

(Received July 5, 2018, Revised May 17, 2019, Accepted June 15, 2019)

Abstract. In this study, the load carrying behavior of piled rafts installed in inclined bearing rock layer was investigated for rock-mounted and -socketed conditions. It was found that settlements induced for an inclined bearing rock layer are larger than for a horizontal layer condition. The load capacity of piled rafts for the rock-mounted condition decreased as rock-layer inclination angle (θ) increased, while vice versa for the rock-socketed condition. The load capacities of raft and piles both decreased with increasing θ for the rock-mounted condition. When bearing rock layer was inclined, loads carried by uphill-side piles were greater than those by downhill-side piles. The values of differential settlements of rock-mounted and -socketed conditions were not significantly different whereas slightly higher for the rock-socketed condition. The values of load sharing ratio (α_p) and its variation with settlement were not markedly changed by the inclination of bedrock. It was shown that α_p for piled rafts installed in rock layer was not affected by θ whereas actual loads carried by raft and piles may vary depending on the pile installation and rock-layer inclination conditions.

Keywords: piled rafts; rock socketed condition, inclined rock layer, load carrying capacity; settlement; load sharing ratio

1. Introduction

Piles are installed often extending to a bedrock layer to support large axial loads from high-rise buildings, bridges and other types of large-scale infrastructures (Horvath and Chae 1989, Leong and Randolph 1994, Zhang and Xu 2009; Al-Omari *et al*. 2016; Khanmohammadi and Fakharian 2018). The types of rock-supported piles can be divided into the cases socketed into or mounted directly on the bedrock layer. Piles of rock-supported condition piles are designed introducing a simplified layering configuration of bearing rock strata, assumed located at certain depth, whereas actual layering condition may be inclined or irregular. For both rock-socketed and -mounted piles in an inclined rock layer, the pile bases of group piles are unevenly located at different depths or with different rock-socket lengths. Such condition would result in asymmetric load distribution within the pile group with changes in the load response and load carrying behavior, which requires further clarification for more enhanced and accurate design.

Many researchers have investigated the load carrying behavior of rock-socketed piles (Reese *et al*. 1969, Horvath *et al*. 1980, Leong and Randolph 1994, Zhang and Xu 2009). Horvath *et al*. (1980) conducted load tests using rock-socketed piles and proposed a design correlation between the rock-socket resistance and uniaxial strength of rock mass. Leong and Randolph (1994) showed that the shaft resistance of soil zone above rock mass layer decreases with increasing rock-socket length. According to Zhang and Xu (2009), as the pile length within soil layer increases, the portion of total load transmitted to the rock-socket zone decreases and load transmitted to the pile base increases with time. Oweis and Hwang (2010) quantified factors for load transferred to rock-socketed micropiles, as affected by rock quality.

The effect of inclined bearing rock layer on the load carrying behavior of foundations has been addressed by several authors. Han and Jiang (2011) suggested the modified bearing capacity factors for shallow foundations resting on an inclined bedrock. For group piles, Xing *et al*. (2014) conducted centrifuge tests to investigate the load carrying behavior of group piles socketed in the inclined bedrock layer. It was found that the load distribution within pile group was not uniform and piles with longer rock-socket length shared more load than those of shorter rock-socket length. Xing *et al*. (2014) also investigated piled rafts of Hezhang Bridge, which was installed on an inclined bedrock layer by approximately 44° and reported that load tended to concentrate on the deeper rock-socketed piles, which was different from those of typical pile groups in soils where the central piles carry more load than surrounding piles. Note that the majority of these previous investigations were targeted on either footings or group piles.

When piles were combined with raft as a piled raft, the load carrying behavior becomes more complicated, due to the pile-raft interactions and the load sharing behavior. In this study, the load carrying behavior of piled rafts installed in an inclined bearing rock layer is investigated focusing on the compared effects and load responses of rock-socked and rock-mounted piles, which was not addressed before. For

*Corresponding author, Professor
E-mail: junlee@yonsei.ac.kr

ISSN: 2005-307X (Print), 2092-6219 (Online)

this purpose, the finite element (FE) analyses were performed considering various configurations of bearing rock-layer inclination and rock-supported conditions. The load response, load sharing behavior and differential settlement are analyzed and compared for the rock-mounted and -socketed cases with rock layer inclination.

2. Load carrying behavior of piles installed on rock

2.1 Load carrying capacity

The load carrying capacity of rock-supported piles has been investigated mainly based on empirical approach and numerical analysis (Leong and Randolph 1994, Carrubba 1997, Han and Jiang 2011). The majority of the methods proposed for predicting the load carrying capacity of rock-supported piles introduced the unconfined compressive strength of rock mass as key design variable. The general formulation of the base resistance for piles bearing on a bedrock layer is given by

$$q_b = f \cdot q_u \tag{1}$$

where q_b = pile base resistance; f = correlation coefficient; and q_u = unconfined compressive strength of rock mass. Rowe and Armitage (1987) presented that q_b is approximately proportional to σ_c with the coefficient equal to 2.7. Zhang and Einstein (1998), on the other hand, indicated that q_b increases non-linearly with σ_c, suggesting the following correlation for drilled shafts in rock

$$q_b = 4.83 q_u^{0.51} \tag{2}$$

While the majority of the proposed correlations have introduced the unconfined compressive strength of intact rock, AASHTO (1989) considered the effect of rock mass defects such as joints and discontinuities as well as the weathering condition of bearing rock layer given as the following design equation

$$q_b = N_{ms} \cdot q_u \tag{3}$$

where N_{ms} = model parameter to consider the rock quality including the shape of rock, joints, and degree of weathering. According to the AASHTO (1989), the effect of rock mass quality on N_{ms} is greater than that of the type of rock. It was presented that the value of N_{ms} for good rock mass quality is 250 times larger than for poor quality rock (AASHTO 1989).

For the skin friction of rock-socketed piles, NAVFAC (1982) suggested the following correlation

$$q_s = (6 \sim 7.9)\left(f_w^{'}\right)^{\frac{1}{2}} \tag{4}$$

where q_s = skin frictional resistance and $f_w^{'}$ = smaller value of unconfined compressive strength of rock and axial compressive strength of concrete. According to Xing *et al*. (2014), there is an optimum rock-socket length, 2.0 times pile diameter, beyond which settlement and base resistance of pile do not change significantly. A more generalized relationship based on the unconfined compression strength of rock can be given as follows

$$q_s = a \cdot q_u^{\ b} \tag{5}$$

where q_u = unconfined compression strength of rock and a and b = correlation parameters. Various values of a and b were proposed (Rosenberg and Journeaux 1976, Horvath and Kenney 1979, Meigh and Wolski 1979, Rowe and Armitage 1978, Zhang and Einstein 1998). Most of these works indicated that the values of a and b are in the ranges of 0.2 to 0.45 and 0.5 to 0.6, respectively.

2.2 Load transfer behavior

For piles socketed into rock, significant portions of applied load are transferred to the rock–pile interface within the rock-socket zone (Carter and Kulhawy 1988, Crapps and Schmertmann 2002, Seol *et al*. 2009). As the frictional resistance of piles is mobilized earlier at smaller settlement, imposed load is first supported by the frictional resistance while the base resistance tends to be mobilized later subsequently and gradually as settlement further increases. According to Carter and Kulhawy (1988), loads carried by pile base are about 10% to 20% of total load for rock-socketed piles. Crapps and Schmertmann (2002) reported higher portion of load carried by pile base, about 30%.

The values of limit settlement, required for the full mobilization of shaft resistance for rock-socketed piles, have been investigated by several authors. Horvath (1982) presented that the shaft resistance is fully mobilized at the settlement of 5.0 mm for large rock-socketed piles. Basarkar and Dewaikar (2006) indicated that the limit settlement is in the range of 5 to 10 mm. Slippage along the shaft takes place once the threshold value of limit settlement exceeds, thereby the pile base begins to carry load further imposed on the pile. According to Zhang and Xu (2009), even if settlement of rock-socketed piles is limited in the 5–15 mm range, a significant portion of total load applied to pile is transmitted to and supported by the rock-socketed pile base and the percentage of total load supported by the rock-socketed pile base increases over time. Note that all studies mentioned herein assumed piles bearing in flat, horizontal rock layer whereas the condition of an inclined bearing rock layer has not been specifically taken into account. The combined foundation type, such as piled rafts, is another issue to be addressed, as the effect of inclined rock-layer configuration may become further changed.

3. Numerical analysis of piled rafts with inclined rock layer

3.1 Finite element modeling

To investigate the load response and load sharing behavior of piled rafts bearing in inclined rock layer, the 3D finite element (FE) analyses were conducted using the commercial FE software PLAXIS 3D FOUNDATION (2008). It should be noted that a piled raft with end-bearing piles installed in a rock layer would show a similar load

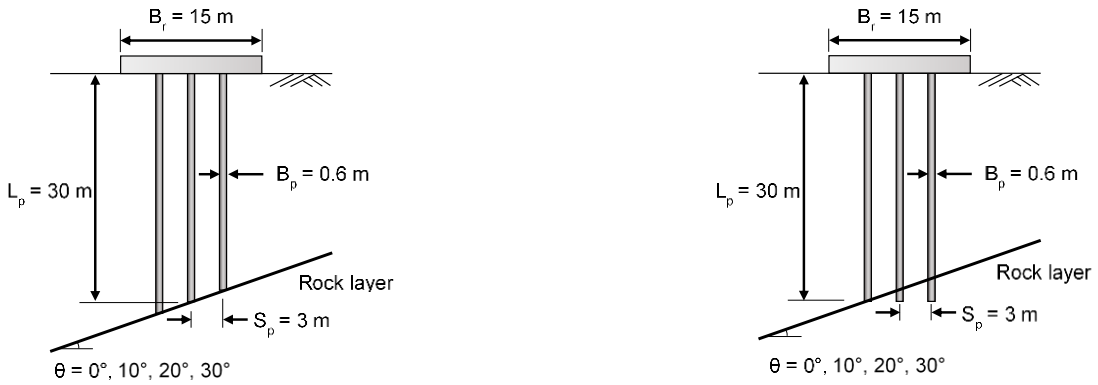

Fig. 1 Configuration of piled rafts (a) mounted on and (b) socketed into inclined rock layer

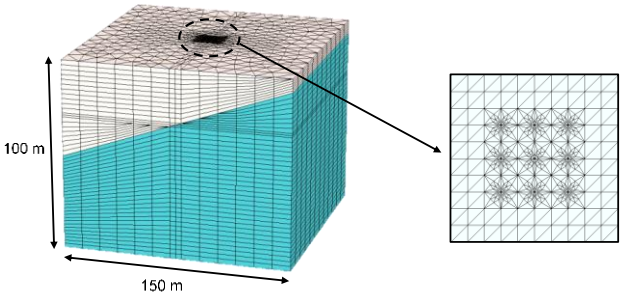

Fig. 2 Finite element model for piled raft with inclined rock layer

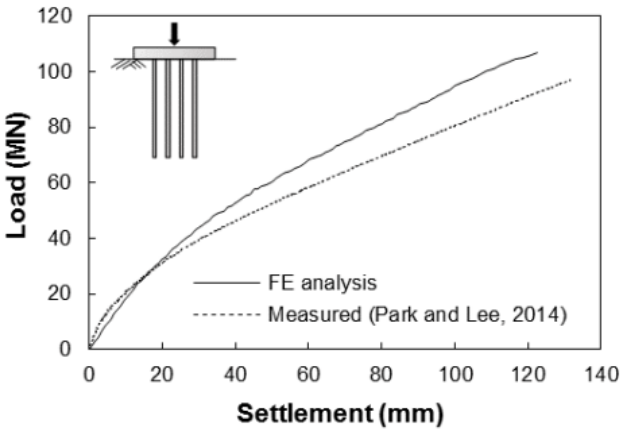

Fig. 3 Measured and calculated load-settlement curves of piled raft

Table 1 Basic properties of soil and rock adopted in FE analyses

Material	D_R (%)	e	γ (kN/m^3)	E (MPa)	ϕ′ (°)	R_{int}	Model
Sand	50	0.63	16.1	37	35	0.7	Mohr-Coulomb
Rock	-	-	27	40000	40	0.84	Mohr-Coulomb

response and load capacity to those of group piles installed in a rock layer due to high end-bearing resistance mobilized from the rock layer. Piled raft foundation was however considered in this study to address a more generalized, actual construction condition as the pile cap of group piles is often installed in contact condition with soils.

The piled-raft model prepared for the FE analyses was composed of a square-shaped raft with the width (B_r) of 15 m and nine piles of 3×3 configuration with the pile spacing of 3 m, corresponding to 5 times the pile diameter (B_p) equal to 0.6 m. The pile length (L_p) was variable as it depended on the type of pile installation in rock, the position of pile within piled raft and the inclination angle of bearing rock layer. Raft and piles were both assumed as a linear elastic material with the elastic modulus and Poisson's ratio equal to 30 GPa and 0.15, respectively.

Fig. 1 shows the detailed configuration of piled rafts and bearing rock layer considered in the FE analyses for rock-mounted [Fig. 1(a)] and rock-socketed [Fig. 1(b)] cases. The inclination angles of bearing rock layer were 0°, 10°, 20°, and 30°. Rock-mounted piles were assumed as directly resting on the bearing rock layer. The lengths of individual piles for such case were then different depending on the inclination angle of bearing rock layer as indicated in Fig. 1(a). For rock-socketed case piles in Fig. 1(b), the lengths of all pile components were the same while the socket lengths of each pile were different depending on the position of pile and inclination angle. The total pile length, the summation of individual pile lengths for piled rafts, were set all the same, equal to 270 m corresponding to the average pile length of 30 m.

Fig. 2 shows the FE model prepared in this study to simulate piled rafts installed in an inclined bearing rock layer. The boundary effects on piled raft can be minimized when whole model is taken with the width of 6 times the raft width, 30 times the pile diameter and the depth of 2 times the pile length (Eid and Shehada 2015, Sinha and Hanna 2017). The width and height of the FE model were 150 and 100 m, respectively, 10 times wider than the raft width and 3.3 times longer than the pile length. The lateral boundaries of the FE model were constrained laterally, allowing only downward movement of soil layers. The bottom boundary was set as a fixed condition. Between piles and soil, the interface condition was introduced, where the interface strength was specified using the strength reduction factor R_{inter} defined as follows

$$c_i = R_{inter} c_{soil} \quad (6)$$

$$\tan\phi_i = R_{inter} \tan\phi_{soil} \le \tan\phi_{soil} \quad (7)$$

where c_i and c_{soil} = cohesive strength of interface and soil; R_{inter} = strength reduction factor; ϕ_i = interface friction angle; and ϕ_{soil} = internal friction angle of soil. For sandy soils, the interface friction angle is in general in the range of 0.5 to 0.8ϕ whereas the interface friction angle within the rock-socketed zone indicates higher values (Hanna and Nguyen 2002, Chaudhary 2007). The values of R_{inter} for the FE analyses in this study were assumed as equal to 0.7 and 0.84 for soil and rock layers, respectively.

3.2 Soil parameters

The soil in the FE analyses was assumed as a medium sand with the relative density of D_R = 50%, void ratio of 0.63 and the unit weight of 16.1 kN/m^3. The Mohr–Coulomb model was adopted to describe the mechanical behavior of soil with the internal friction angle of 35°. To consider the stress-dependent variation of elastic modulus with depth, the correlation proposed by Hardin and Black (1966) was introduced, given by the following relationship

$$G_0 = C_g \frac{\left(e_g - e_0\right)}{1+e_0} P_A^{\left(1-n_g\right)} \left(\sigma'_m\right)^{n_g} \quad (8)$$

where G_0 = initial shear modulus; C_g, e_g and n_g = correlation parameters; e_0 = initial void ratio; P_A = reference pressure = 100 kPa; and σ'_m = mean effective stress. The values of C_g, e_g and n_g for the assumed sand were 612, 2.17 and 0.44, respectively (Salgado *et al*. 2000). The depth variation of soil stiffness was then taken into account through the values of σ'_m that increase with depth indicating higher confining stress. The Poisson's ratio was equal to 0.3.

The rock mass rating (RMR) system was adopted to estimate input properties of bearing rock using the following correlations (Bieniawski 1978, Serafim and Periera 1983)

$$E_m = 2RMR - 100 \quad (9)$$

$$E_m = 10^{(RMR-10)/40} \quad (10)$$

where E_m = elastic modulus of rock mass in the unit of GPa, and RMR = rock mass rating = dimensionless value from 0 to 100. Eqs. (9)-(10) were proposed by Bieniawski (1978) and Serafim and Periera (1983) for RMR greater and smaller than 50, respectively. The value of RMR for the bearing rock layer considered in the FE analyses was 74, a representative value for soft rocks (Bieniawski 1973). Other detailed input parameters adopted in the FE analyses are given in Table 1. As strength and stiffness were target properties to distinguish soil and rock, the Mohr-Coulomb model was adopted in this study to model both soil and rock using different values of stiffness and strength were used as main input variables.

3.3 Validation of analysis

To check the validity of the FE analyses prepared and performed in this study, a case example was selected from the literature and adopted to compare measured and estimated load responses of piled rafts. Park and Lee (2015) conducted the centrifuge load test using a model piled raft installed in sand. The model piled raft had a 9-m square raft and 16 piles of 4×4 configuration with the diameter (B_p), length (L_p) and spacing (S_p) of 0.6, 15 and 2.4 m, respectively. This pile spacing corresponds $4B_p$. The test soil was silica sand with the maximum and minimum unit weights ($Y_{d,max}$, $Y_{d,min}$), coefficient of uniformity (C_u), mean grain diameter (D_{50}), critical-state and peak friction angles (ϕ'_{crit} and ϕ'_p) of 16.12 kN/m^3, 12.19 kN/m^3, 1.96, 0.21 mm, 33°, and 43°, respectively. The values of elastic modulus with depth were obtained using Eq. (8). Other modeling procedure for the FE analysis was the same as described in the previous section.

The load-settlement curves obtained from the FE analysis and measured from the centrifuge test were plotted in Fig. 3. The FE result showed more or less overestimated load response, which became more pronounced as settlement increased. Nonetheless, the compared results in Fig. 3 between the measured and calculated load responses indicated reasonably close agreement.

A piled raft installed in sand was adopted in this validation because cases of instrumented field load tests using full- and large-scaled piled rafts installed in rock was hardly reported. By introducing and comparing results from actual load test using a piled raft in sand, it was intended that the minimum level of required validity for the FE simulation of piled raft was to be ensured.

4. Compared load responses of rock-supported piled rafts

4.1 Load-settlement curves

The load-settlement curves of piled rafts with the rock-mounted and -socketed conditions obtained from the FE analyses are shown in Fig. 4 for different rock-layer inclination angles (θ). For piled rafts mounted on rock layer in Fig. 4(a), the load carrying capacity decreased as θ increased. Within the initial settlement range up to approximately 1 mm, the load responses were all similar without noticeably significant effect of rock layer inclination. Beyond this initial settlement range, the load-settlement behavior of piled rafts became different depending on the value of θ. The load carrying capacity for the inclined rock-layer case was smaller than for the flat, horizontal rock-layer case with θ = 0° that bounded the upper range of load-settlement curves. The smaller load carrying capacity for higher θ is due to the unsymmetrical pile length configuration as settlement and deformation of longer piles become larger, dominating the overall load carrying capacity.

For piled rafts socketed into rock layer in Fig. 4(b), the load carrying capacity increased as θ increased, which was different from the rock-mounted case in Fig. 4(a). As compared to the rock-mounted case, less changes in the load-settlement curve were observed with increases in θ. The load responses were stiffer for higher θ, which

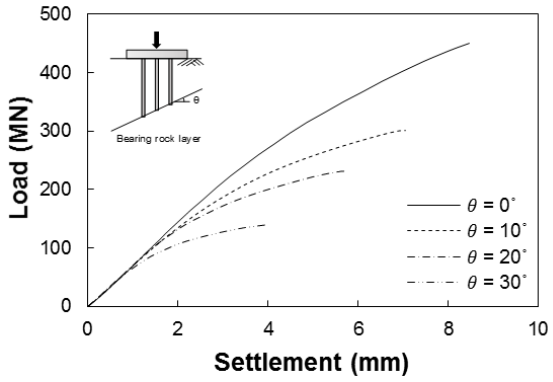

(a)

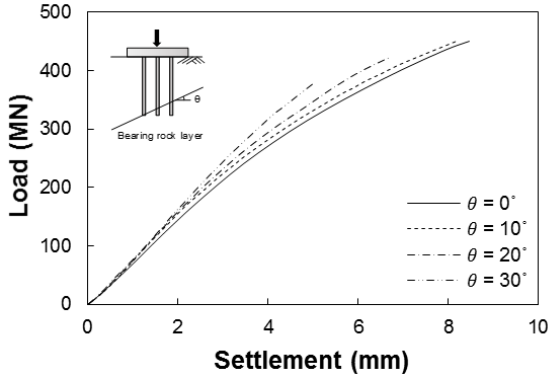

(b)

Fig. 4 Load settlement curves of piled rafts (a) mounted and (b) socketed into rock for different θ

indicated longer socket length and higher mobilized frictional resistance within the rock socket zone. Note that less changes in the load-settlement curve with θ for rock-socketed piled rafts is consistent with the existence of limit socket resistance, which indicates that the socket resistance does not increase proportionally to rock-socket length (Seo *et al*. 2013, Xing *et al*. 2014).

From the load-settlement curves in Fig. 4, the load carrying capacities of piled rafts for the inclined rock-layer condition were obtained and compared with those for the horizontal rock-layer condition of θ = 0°. For this purpose, the load-capacity ratio ξ_{pr} was defined and adopted into the comparison, given as the following relationship

$$\xi_{pr} = \frac{Q_{pr,i}}{Q_{pr}} \tag{11}$$

where ξ_{pr} = load capacity ratio of inclined to horizontal rock-layer conditions; $Q_{pr,i}$ and Q_{pr} = load capacities of piled rafts for inclined and horizontal rock-layer conditions. The load capacity in this comparison was specified at the settlement of 4 mm, considering the rock-supported condition (Ng *et al*. 2001). As the failure condition is hardly achieved or observed from a rock-embedded condition, the settlement-based criterion was adopted to define the load capacity of piled raft foundations in this study. Fig. 5 shows the values of ξ_{pr} for the rock-mounted and rock-socketed piled rafts. For the rock-mounted case, the values of ξ_{pr} decreased as θ increased. The largest reduction in the load

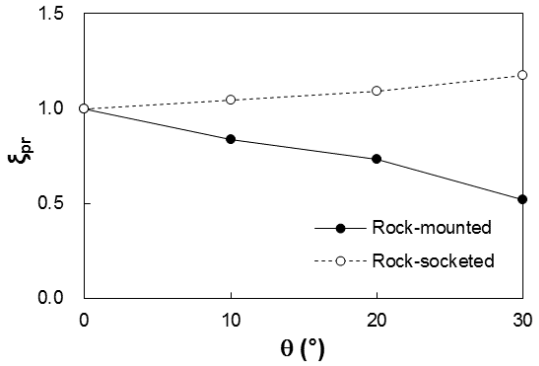

Fig. 5 Changes in ξ_{pr} with inclination angle θ

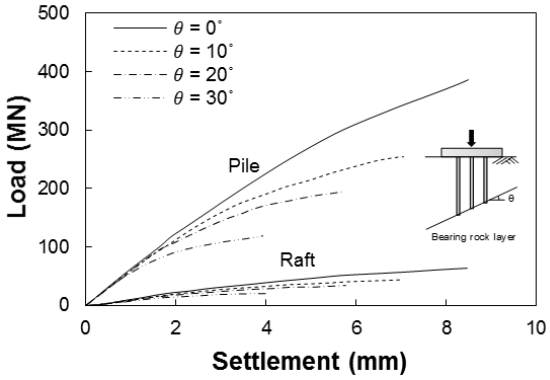

(a)

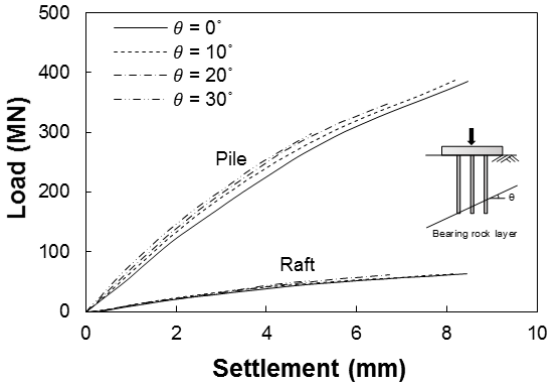

(b)

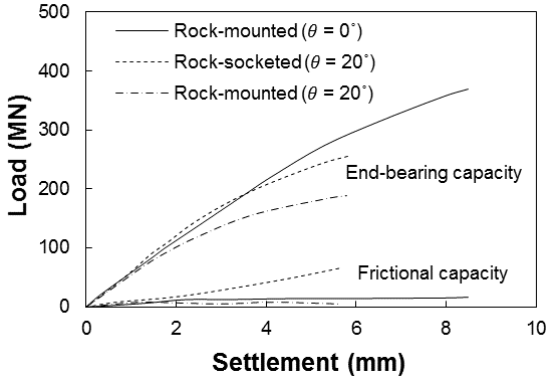

(c)

Fig. 6 Decomposed load-settlement curves of raft and pile components for (a) rock-mounted; (b) -socketed conditions with inclined rock layer and (c) decomposed end-bearing and frictional components

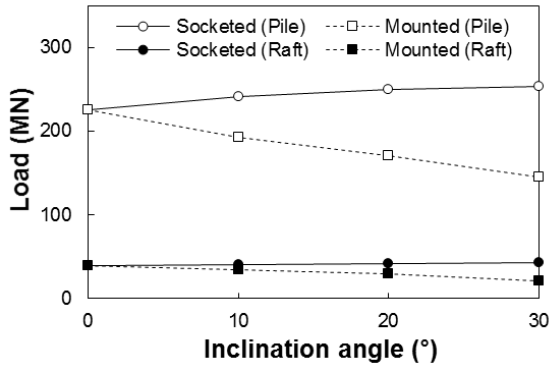

Fig. 7 Values of loads shared by raft and piles for rock-mounted and -socketed conditions

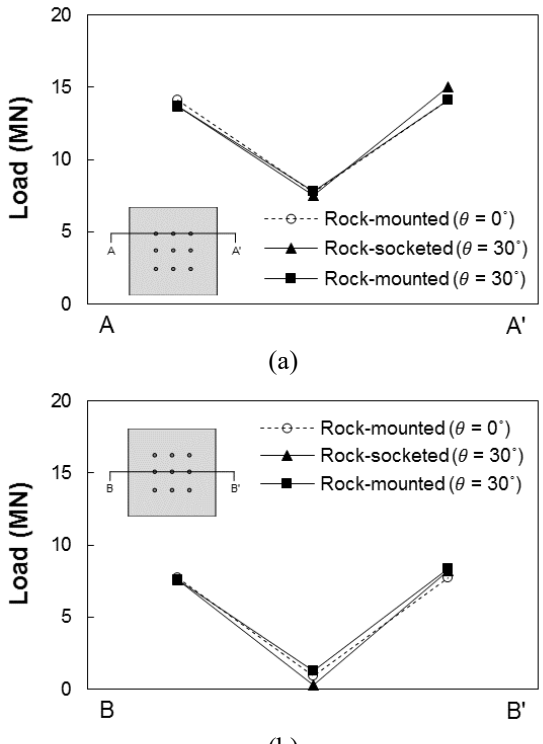

Fig. 8 Load distributions on piles of piled raft for cross-sections of (a) A-A′ and (b) B-B′

capacity of 48 % was observed for θ = 30°. For the rock-socketed case, ξ_{pr} increased up to 17% with increasing θ. These results indicate that the inclined rock-layer condition can affect positively or negatively the load carrying behavior of piled rafts depending of the installation method.

4.2 Decomposed load responses

The decomposed load-settlement curves of raft and pile components for piled rafts were obtained from the FE analyses and plotted in Fig. 6 for the rock-mounted [Fig. 6(a)] and rock-socketed [Fig. 6(b)] conditions with different θs. The load-settlement curves of piles were also decomposed into end-bearing and friction components as plotted in Fig. 6(c). The end-bearing capacities for all cases were much higher than the frictional shaft capacities. As shown in Fig. 6(a) for the rock-mounted condition, the load carrying capacities of raft and piles both decreased with increasing θ. However, the decomposed load-settlement curves of piles showed more changes with θ than those of raft. This confirms that piles control the load capacity of piled rafts mounted on inclined rock layers whereas the load response of raft indicates minor effect.

The decomposed load-settlement curves of raft and piles for the rock-socketed condition in Fig. 6(b) showed less variation with θ than for the rock-mounted condition. While the rock-socket length of piles increased with θ, the lengths of individual piles were all equal, different from the rock-mounted cases. This in turn represents that the load carrying capacities of rock-socketed piles may not be significantly different, if the pile lengths of individual piles are equal.

Based on the decomposed load-settlement curves in Fig. 4, the values of loads carried by raft and piles are obtained and compared in Fig. 7 for the rock-mounted and -socketed cases with θ. For the rock-mounted piled rafts, loads carried by raft and piles both decreased as θ increased. For the rock-socketed piled rafts, however, loads carried by raft and piles increases with increasing θ, due to increases in the rock socket length.

5. Effects of inclined bearing rock layer

5.1 Load distribution on piles

The distribution of loads imposed on individual piles of piled raft were obtained and compared for the rock-mounted and -socketed cases with the inclined rock layer in Fig. 8. Two sections of A-A' and B-B' for piles along the edge and middle rows were considered and adopted into the comparison in Figs. 8(a) and 8(b), respectively. The results for θ = 0° were also obtained and included in Fig. 8 for comparison. The values of total load considered for each case in Fig. 8 were all the same as equal to 100 MN.

As shown in Fig. 8, loads carried by center pile were smallest. For θ = 0°, the symmetrical load distribution was observed with the values of loads equal to 0.9, 7.7 and 14.1 MN for the center, edge and corner piles, respectively. For the inclined condition, the load distributions were not noticeably different from those of the horizontal case of θ = 0°. Nonetheless, when the bearing rock layer was inclined, loads carried by the uphill-side piles were greater than those carried by the downhill-side piles for both rock-mounted and -socketed cases. While these results were obtained from the FE analyses, similar results can be found from the field test case of Roh *et al.* (2019) where the similar unsymmetrical load distribution of piled raft in an inclined rock layer was reported. It was also observed that the loads imposed on the uphill-side piles for the rock-socketed case were slightly larger than for the rock-mounted case, which can be attributed to the mobilized rock-socket resistance. The loads imposed on the downhill-side piles were however similar as no socketed condition was involved for both cases. These results confirm that the resistance mobilized along the rock-socket zone is the main component that contributes to the higher load capacity of rock-socketed piled rafts than of rock-mounted case for the inclined rock layer condition.

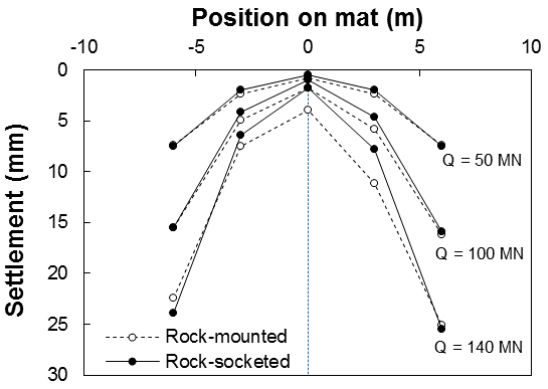

(a)

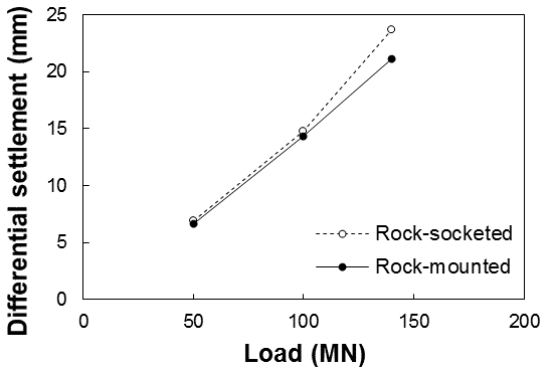

(b)

Fig. 9 Differential settlements of rock-mounted and -socketed piled rafts with (a) position on raft and (b) value of applied load

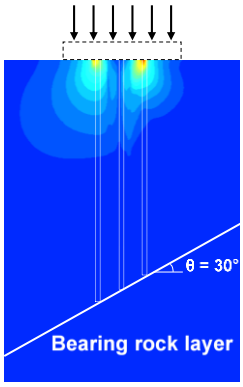

(a)

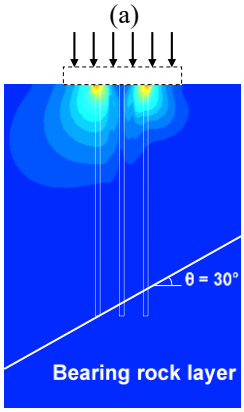

(b)

Fig. 10 Displacement contour plots of (a) rock-mounted and (b) -socketed cases

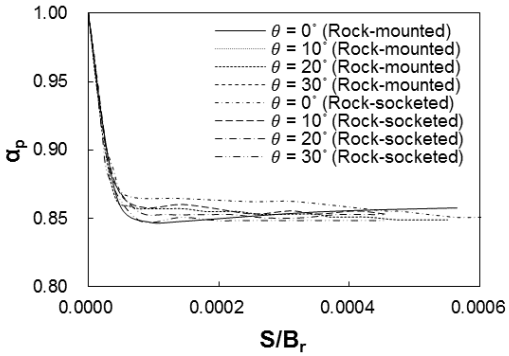

Fig. 11 Values of load sharing ratio with settlement for piled rafts mounted and socketed into rock layer for different θs

5.2 Differential settlement

The horizontal profiles of induced settlement along the cross-section of piled rafts and the values of different settlement with load were obtained and plotted in Figs. 9(a) and 9(b), respectively, for the inclined rock-layer condition of θ = 30°. The results were compared for the rock-mounted and -socketed conditions. For all cases, the smallest settlements were induced from the center piles whereas the uphill-side corner piles indicated the largest settlements. As piles were all bearing in rock layers as either mounted or socketed, differences in settlements between the uphill- and downhill-side piles were not significantly large. However, differential settlements between the center and corner piles were quite noticeable, which increased with increasing load. From Fig. 9(b), it is seen that the values of differential settlement increased as load increased. The values of differential settlement for the rock-mounted and -socketed conditions were not significantly different for low range of load level whereas the rock-socketed case tends to produce slightly higher different settlement as the load level becomes higher.

Fig. 10 shows the contour plots of displacement fields compared for rock-mounted and -socketed piles on inclined bearing rock layer with θ = 30°. As compared in Fig. 10(a) and 10(b), the uphill-side rock-socketed piles in Fig. 10(b) show less induced settlement than for those of the rock-mounted condition in Fig. 10(a), which explains the larger differential settlement for the rock-socketed condition.

5.3 Load sharing ratios

Based on the load variation with θ in Fig. 6 and the decomposed load-settlement curves in Fig. 5, the values of load sharing ratio (α_p) were obtained for both rock-mounted and -socketed cases. These were plotted in Fig. 11 for different θs as a function of settlement. As the load capacity of smaller-diameter piles is mobilized earlier than that of larger-sized raft, α_p is higher initially and then decreases non-linearly with increasing settlement, converging to a certain value depending on the number of piles and pile size.

From Fig. 11, it is seen that the values of α_p and its variation with settlement were similar for both rock-mounted and -socketed cases, indicating no significant

effect of the rock-layer inclination. As previously discussed and shown in Fig. 6, the magnitudes of loads carried by raft and piles were different for the rock-mounted and -socketed conditions, and were affected by the inclination angle of bearing rock layer. However, the ratios of increased and decreased loads of raft and piles were similar irrespective of the rock-supported type and bearing rock-layer inclination. These results indicate that, if piles are contact with rock at the base, the load sharing ratio remains virtually the same whereas the load carrying behavior of individual foundation component may vary depending on the installation and rock-layer conditions.

6. Conclusions

In this study, the load carrying behavior of piled rafts installed in an inclined bearing rock layer was investigated based on the results from the finite element (FE) analyses, focusing on the load carrying behaviors of rock-mounted and rock-socked piles and the effect of rock-layer inclination. When bearing rock-layer was inclined, the load carrying capacity of rock-socketed piled rafts was higher than of rock-mounted piled rafts. The load capacity of piled rafts with the rock-mounted condition decreased as the rock-layer inclination angle (θ) increased, due to the unsymmetrical pile length configuration. For piled rafts with the rock-socketed condition, the load capacity increased with increasing θ, due to longer rock-socket length and thus higher rock-socket frictional resistance. Less changes in the load-settlement curve were observed with increasing θ, which was consistent with the existence of limit socket resistance.

The load capacities of raft and piles for rock-mounted piled rafts both decreased with increasing θ, which was mainly caused by reductions in pile load capacity. For rock-socketed piled rafts, less variation in pile and raft load capacities with θ was observed. For all cases, loads carried by center piles were smallest. When the bearing rock layer was inclined, loads carried by the uphill-side piles were greater than those carried by the downhill-side piles for both rock-mounted and rock-socketed cases. The values of differential settlements of rock-mounted and -socketed cases were not significantly different whereas the rock-socketed case produced slightly higher differential settlements.

The values of load sharing ratio (α_p) were all similar for both rock-mounted and rock–socketed cases and no significant effect of the rock-layer inclination was observed. While loads carried by raft and piles were different, the ratios of the loads carried of raft and piles were similar irrespective of rock-supported condition and rock-layer inclination. This indicates that, if piles are installed in a rock layer, the load-sharing ratio of piled rafts remains virtually the same whereas the load carrying behavior of raft and individual piles may vary depending on the pile installation and rock-layer inclination conditions.

Acknowledgments

This work was supported by the Korea Institute of Energy Technology Evaluation and Planning (KETEP), the Ministry of Trade, Industry and Energy (MOTIE) and the National Research Foundation of Korea (NRF) of the Republic of Korea (Nos. 2016R1D1A1A09919098 and 20194030202460).

References

AASHTO (1989), *Standard Specifications for Highway Bridges*, American Association of State Highway and Transportation Officials, Washington, U.S.A.

Al-Omari, R.R., Al-Azzawi, A.A. and Al-Abbas, K.A. (2016), "Behavior of piled rafts overlying a tunnel in sandy soil", *Geomech. Eng.*, **10**(5), 599-615. http://dx.doi.org/10.12989/gae.2016.10.5.599.

Basarkar, S.S. and Dewaikar, D.M. (2006), "Load transfer characteristics of socketed piles in Mumbai region", *Soils Found.*, **46**(2), 247-257. https://doi.org/10.3208/sandf.46.247.

Bieniawski, Z.T. (1973), "Engineering classification of jointed rock masses", *Civ. Eng. South Africa*, **15**(12), 335-343.

Bieniawski, Z.T. (1978), "Determining rock mass deformability-experiences from case histories", *Int. J. Rock Mech. Min. Sci. Geomech. Abstr.*, **15**(5), 237-247. https://doi.org/10.1016/0148-9062(78)90956-7.

Carrubba, P. (1997), "Skin friction on large-diameter piles socketed into rock", *Can. Geotech. J.*, **34**(2), 230-240. https://doi.org/10.1139/t96-104.

Carter, J.P. and Kulhawy, F.H. (1988), "Analysis and design of drilled shaft foundations socketed into rock", Report No. EL-5918, Electric Power Research Institute, Palo Alto, California, U.S.A.

Chaudhary, M.T.A. (2007), "FEM modelling of a large piled raft for settlement control in weak rock", *Eng. Struct.*, **29**(11), 2901-2907. https://doi.org/10.1016/j.engstruct.2007.02.001.

Crapps, D.K. and Schmertmann, J.H. (2002), "Compression top load reaching shaft bottom-theory vs. tests", *Proceedings of the International Deep Foundations Congress 2002*, Orlando, Florida, U.S.A., February.

Eid, H.T. and Shehada, A.A. (2015), "Estimating the elastic settlement of piled foundations in rock", *Int. J. Geomech.*, **15**(3), 04014059. https://doi.org/10.1061/(ASCE)GM.1943-5622.0000376.

Han, J. and Jiang, G. (2011), "Influence of inclined bedrock on undrained bearing capacity of shallow strip foundations", *Proceedings of the Geo-Frontiers Congress 2011*, Dallas, Texas, U.S.A., March.

Hanna, A.M. and Nguyen, T.Q. (2002), "An axisymmetric model for ultimate capacity of a single pile in sand", *Soils Found.*, **42**(2), 47-58. https://doi.org/10.3208/sandf.42.2_47.

Hardin, B.O. and Black, W.L. (1966), "Sand stiffness under various triaxial stresses", *J. Soil Mech. Found. Div.*, **92**(2), 27-42.

Horvath, R.G. (1982), "Drilled piers socketed into weak shale: methods of improving performance", Ph.D. Dissertation, University of Toronto, Toronto, Canada.

Horvath, R.G. and Chae, K.J. (1989), "Long-term settlement of model rock-socketed piers", *Can. Geotech. J.*, **26**(3), 348-358. https://doi.org/10.1139/t89-049.

Horvath, R.G., Kenny, T.C. and Trow, W.A. (1980), "Results of tests to determine shaft resistance of rock-socketed drilled piers", *Proceedings of the International Conference on Structural Foundations on Rock*, Sydney, Australia, May.

Khanmohammadi, M. and Fakharian, K. (2018), "Evaluation of performance of piled-raft foundations on soft clay: A case study", *Geomech. Eng.*, **14**(1), 43-50. https://doi.org/10.12989/gae.2018.14.1.043.

Leong, E.C. and Randolph, M.F. (1994), "Finite element modelling of rock-socketed piles", *Int. J. Numer. Anal. Meth. Geomech.*, **18**(1), 25-47. https://doi.org/10.1002/nag.1610180103.

NAVFAC (1982), *Foundations and Earth Structures Design Manual 7.2*, Navy Facilities Engineering Command; Alexandria, Virginia, U.S.A.

Ng, C.W.W., Yau, T.L.Y., Li, J.H.M. and Tang, W.H. (2001), "Side resistance of large diameter bored piles socketed into decomposed rocks", *J. Geotech. Geoenviron. Eng.*, **127**(8), 642-657. https://doi.org/10.1061/(ASCE)1090-0241(2001)127:8(642)

Oweis, I. and Hwang, J. (2010), "Load transfer to micro pile rock socket", *Proceedings of GeoFlorida 2010*, Orlando, Florida, U.S.A., February.

Park, D. and Lee, J. (2015), "Comparative analysis of various interaction effects for piled rafts in sands using centrifuge tests", *J. Geotech. Geoenviron. Eng.*, **141**(1), 04014082. https://doi.org/10.1061/(ASCE)GT.1943-5606.0001183.

PLAXIS (2008), *PLAXIS 3D Foundation Version 2.0 Manual*, Plaxis BV, Netherlands.

Reese, L.C., Hudson, W.R. and Vijayvergiya, V.N. (1969), "An investigation of the interaction between bored pile and soil", *Proceedings of 7th International Conference on Soil Mechanics and Foundation Engineering*, Mexico City, Mexico.

Roh, Y., Kim, G., Kim, I., Kim, J., Jeong, S. and Lee, J. (2019), "Lessons learned from field monitoring of instrumented piled raft bearing in rock layer", *J. Geotech. Geoenviron. Eng.*, **145**(8), 05019005. https://doi.org/10.1061/(ASCE)GT.1943-5606.0002078.

Rowe, R.K. and Armitage, H.H. (1987), "A design method for drilled piers in soft rock", *Can. Geotech. J.*, **24**(1), 126-142. https://doi.org/10.1139/t87-011.

Salgado, R., Bandini, P. and Karim, A. (2000), "Shear strength and stiffness of silty sand", *J. Geotech. Geoenviron. Eng.*, **126**(5), 451-462. https://doi.org/10.1061/(ASCE)1090-0241(2000)126:5(451)

Seo, H., Prezzi, M. and Salgado, R. (2013), "Instrumented static load test on rock-socketed micropile", *J. Geotech. Geoenviron. Eng.*, **139**(12), 2037-2047. https://doi.org/10.1061/(ASCE)GT.1943-5606.0000946.

Seol, H., Jeong, S. and Cho, S. (2009), "Analytical method for load-transfer characteristics of rock-socketed drilled shafts", *J. Geotech. Geoenviron. Eng.*, **135**(6), 778-789. https://doi.org/10.1061/(ASCE)1090-0241(2009)135:6(778).

Serafim, J.L. and Pereira, J.P. (1983), "Consideration of the geomechanical classification of Bieniawski", *Proceedings of the International Symposium on Engineering Geology and Underground Constructions*, Lisbon, Portugal.

Sinha, A. and Hanna, A.M. (2917), "3D numerical model for piled raft foundation", *Int. J. Geomech.*, **17**(2), 04016055. https://doi.org/10.1061/(ASCE)GM.1943-5622.0000674.

Xing, H., Zhang, Z., Meng, M., Luo, Y. and Ye, G. (2014), "Centrifuge tests of superlarge-diameter rock-socketed piles and their bearing characteristics", *J. Bridge Eng.*, **19**(6), 04014010. https://doi.org/10.1061/(ASCE)BE.1943-5592.0000582.

Zhang, L. and Einstein, H. (1998), "End bearing capacity of drilled shafts in rock", *J. Geotech. Geoenviron. Eng.*, **124**(7), 57-58. https://doi.org/10.1061/(ASCE)1090-0241(1998)124:7(574).

Zhang, L. and Xu, J. (2009), "Axial load transfer behavior of rock-socketed shafts", *Proceedings of the International Foundation Congress and Equipment Expo 2009*, Orlando, Florida, U.S.A., March.